Journal of the Korean Society of Oceanography
Vol. 37, No. 1, pp. 10 — 19 March 2002

Tidal Front in the Main Tidal Channel of Kyunggi Bay, Eastern Yellow Sea

HEUNG-JAE LEE, SEOK LEE, CHEOL-HO CHO AND CHEOL-HO KIM
National Research Laboratory for Ocean Prediction of the Yellow and East China Seas
Korea Ocean Research and Development Institute, P.O. Box 29, Ansan, 425-600, Korea

The detailed structure of a tidal front and its ebb-to-flood variation in the main tidal channel of the Kyunggi Bay in the mid-west coast of Korea were investigated by analyzing CTD data and drifter trajectories collected in late July 1999. A typical tidal front was formed in water about 60 m deep at the mouth of the channel. Isotherms and isohalines in the upper layer above the seasonal pycnocline in the offshore stratified zone inclined upward to the sea surface to form a surface front, while those in the lower layer declined to the bottom to create a bottom front. The location of the front is consistent with 100 s^3/cm^2 of the mixing index H/U^3 defined by Simpson and Hunter (1974), where H is the water depth and U is the amplitude of tidal current. The potential energy anomaly in the frontal zone varied at an ebb-to-flood tidal cycle, showing a minimum at slack water after ebb but a maximum at slack water after flood. This ebb-to-flood variation in potential energy anomaly is not accounted for by the mixing index. We conclude that on- and offshore displacement of the water column by tidal advection is responsible for the ebb-to-flood variation in the frontal zone.

Key words: Tidal front, Mixing index, Potential energy anomaly, Kyunggi Bay, Yellow Sea

INTRODUCTION

The Kyunggi Bay is a large estuary located in the mid-west coast of Korea and includes well-developed tidal channels and small tributaries. The largest of the tidal channels is located in the southern part of the bay and extends about 100 km from the Inchon Harbor to the Yellow Sea along the southern coast (Fig. 1). This channel is hereinafter referred to as the main channel. Estuarine water in the bay flows through the main channel toward the Yellow Sea, while offshore water in the Yellow Sea flows into the bay, since the channel acts as a unique pipeline connecting small estuaries in the bay and the Yellow Sea. The estuarine and offshore waters consequently meet somewhere in the channel to eventually form a front.

Tides in the Kyunggi Bay are the largest in the Yellow Sea, with a spring tidal range of about 8 m near the Inchon Harbor (Yi, 1972). Tidal currents exceed 1.5 m/s near the Inchon Harbor located in the inner part of the channel (National Oceanographic Research Institute of Korea, 1998) and are about 1 m/s even at the mouth of the channel. This prominent tidal current may play an important role in material transport and water exchange in the bay. In the absence of strong tidal current, dense offshore water intrudes into the lower layer and light estuarine water flows out through the upper layer, forming a wedge-shaped front (Officer, 1976). When there is strong tidal current, the wedge-shaped front hardly remains since nonlinear interactions between the tidal current and bottom topography enhance vertical mixing (Simpson and Hunter, 1974).

Lie (1989) observed that the mean location of tidal fronts in the Yellow Sea is fairly consistent with 100 $s^3\,m^{-2}$ of the Simpson-Hunter mixing parameter H/U^3, where H is the water depth and U is the amplitude of tidal current. The appearance of cold surface water north of the Taean peninsula in the southern part of the bay during summer was attributed to tidal mixing (Lie, 1989; Cho and Seung, 1989; Choi *et al.*, 1998). Seung *et al.* (1990) and Choi and Park (1998) also observed the appearance of cold water and that isotherms and isohalines in the inner part of the main tidal channel are vertically erected during summer.

*Corresponding author: hjlie@kordi.re.kr

Despite the important role of the main tidal channel for water exchange and material transport, detailed oceanographic structures in the main tidal channel have yet to be investigated in terms of tidal mixing. To describe the effect of tidal mixing on the bay's hydrographic structure, we conducted physical and chemical observations in late July 1999. In this study, we will investigate hydrographic structures along the channel in the main tidal channel and also examine hourly variations of stratification by analyzing CTD data and drifter trajectories observed in the tidal frontal zone.

DATA COLLECTION

Fig. 1 presents our study area and bottom topography in meters. The main tidal channel consists of the outer and inner channels. The inner channel has two navigational passages. The channel geometry is characterized by abrupt bathymetric changes associated with shallow shoals and smaller estuaries annexed to the channel. Oceanographic structures in the channel may vary not only in space due to the uneven distribution of tidal currents and bottom topography, but also in time due to temporal variation of tidal currents.

For the hydrographic structure along the channel, we collected CTD data at fourteen stations approximately along the central axis from July 26 to 29, 1999. Of the fourteen stations, five were located in the southern passage of the inner channel which was shallower than 50 m (stations K03 to K07), and nine were in the middle and outer channel which was deeper than 50 m (stations K02 to C05). The observations were made on July 26 for stations K01 to K07 and on July 29 for the other stations owing to

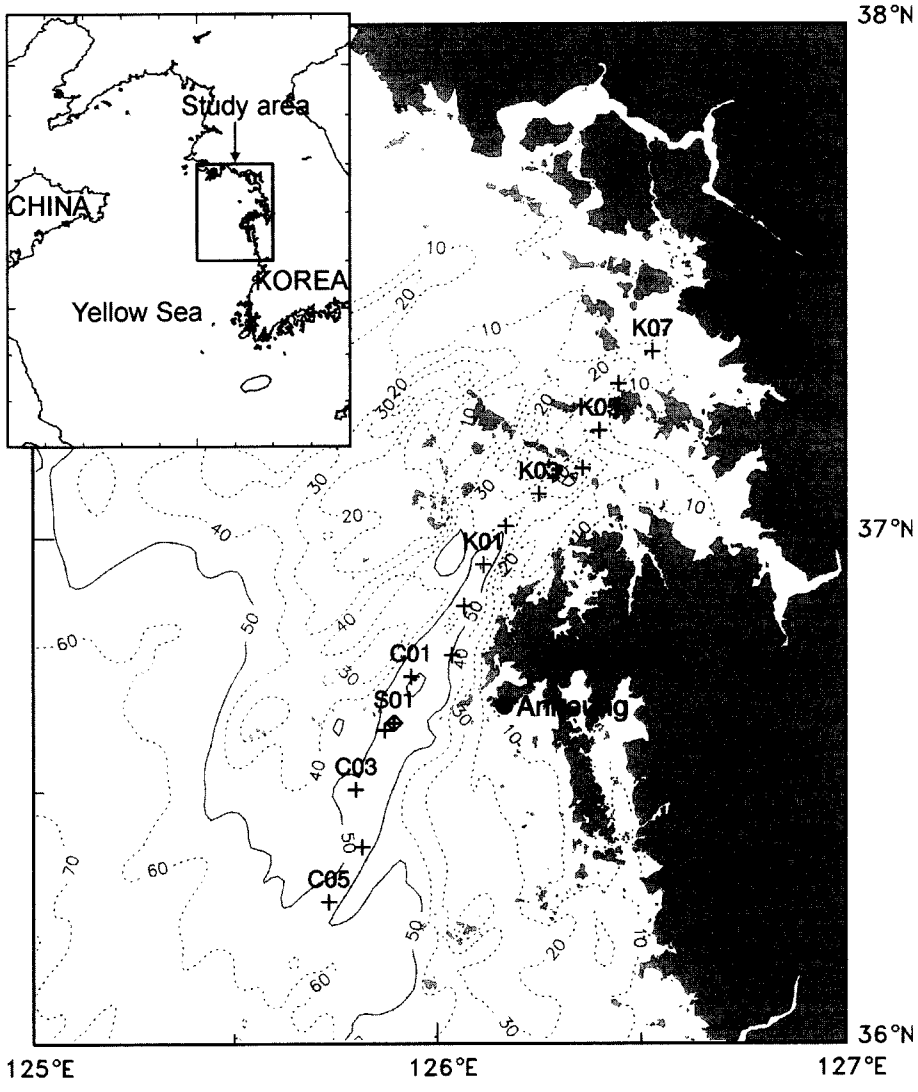

Fig. 1. Study area in the Kyunggi Bay and bottom topography in meters. Crosses denote CTD stations. At station S01, two GPS drifters were deployed and CTD castings were made at one-hour intervals for 13 hours starting 7:30 July 25, 1999.

typhoon Neil. We made CTD casts at station S01 thirteen times at about one-hour intervals on July 25 and 26 in order to examine the response of water column structure in the tidal frontal zone to the hourly variation of tidal currents. CTD data were collected using a SeaBird 9/11 system and were subsampled every one meter by averaging all the data contained within 20 cm of each computation depth.

Current measurements using the current meter mooring and trawl-resisted bottom mounting system in the main channel are ultimately difficult, since the channel serves as the main navigation route to the Inchon Harbor, and also since the sea bed is covered with soft sediments of sand and muddy sand (Park *et al.*, 1994). To circumvent this, we operated a ship-mounted acoustic Doppler current profiler (ADCP) during hourly CTD measurements at station S01 and released two Global Positioning System (GPS) drifters equipped with holey-sock drogues of World Ocean Circulation Experiment (WOCE) prototype centered 15 m and 40 m below the sea surface. ADCP data were not subjected to analysis due to unstable heading values. Positions of the drifters were fixed every two minutes and were smoothed by a 22-minute (eleven positions) moving average to remove high frequency fluctuations.

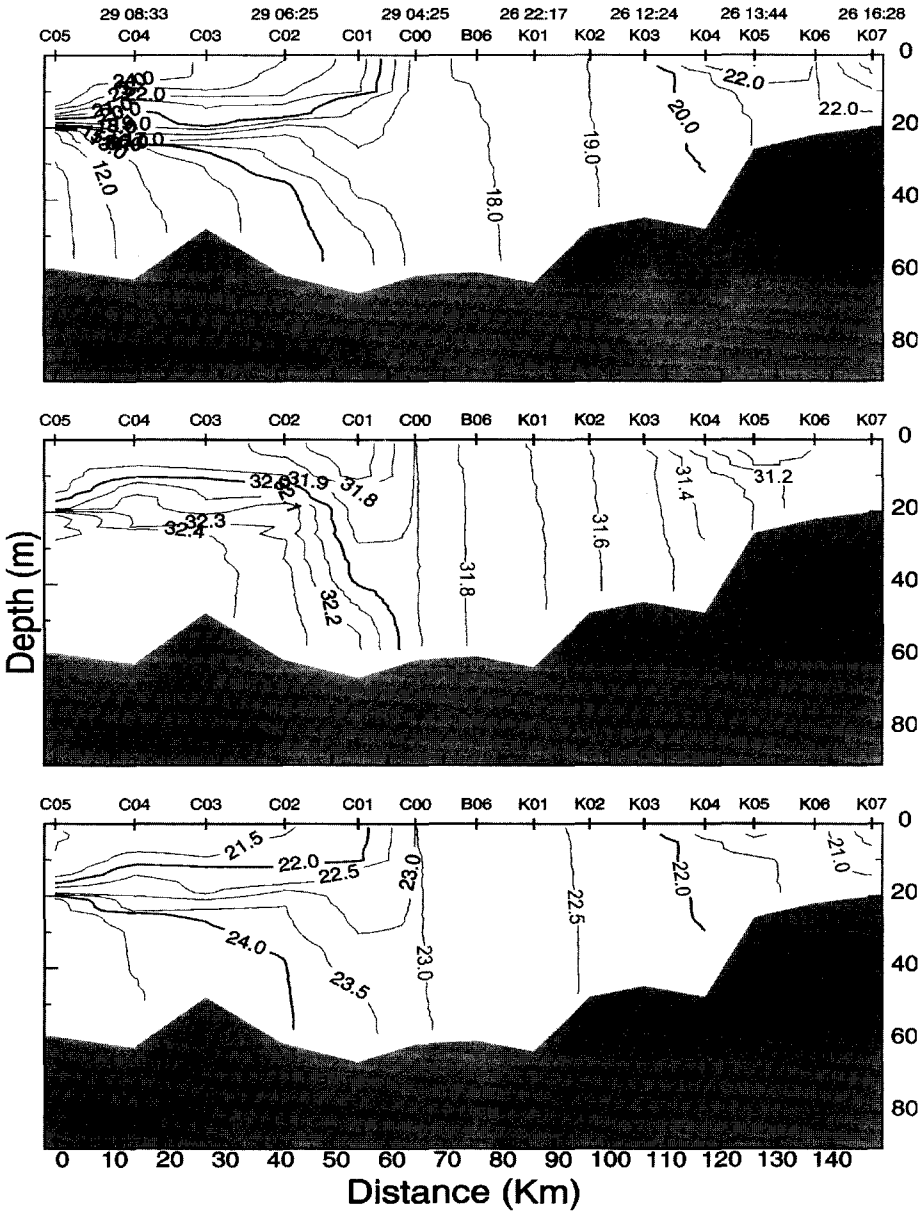

Fig. 2. Vertical sections of temperature, salinity, and sigma-t in the main tidal channel observed from July 26 to 29, 1998. Surface and bottom fronts are located near station C01. Observation time is marked in the upper panel.

HYDROGRAPHIC STRUCTURES ALONG THE CHANNEL

Temperature, salinity and density

Fig. 2 presents vertical sections of temperature, salinity and sigma-t in the direction along the channel. Since the CTD observations were made on July 26 and 29 (lunar calendar: June 14 and 17), temperature and salinity on July 26 and 29 may have changed primarily due to the spring-neap tide cycle. The observations were made during the spring tide period, so radical changes in the vertical structures were unlikely. The vertical sections clearly show the formation of pronounced fronts at the sea surface and the bottom near station C01, where the seasonal thermocline and pycnocline were destroyed. The channel can be classified into three types according to degree of stratification. The first type is a weakly stratified zone in the shallow inner channel (stations K03-K07). The second is a strongly stratified zone in the outer channel (stations C01-C05) where a two-layered structure was well established. The third is a well-mixed zone in the middle channel 50 to 65 m deep (stations C00-K03).

Salinity in the inner channel frequently drops to below 30.0 psu during summer when discharge from the Han River increases (e.g., Seung *et al.*, 1990, Fig. 3). However, in the course of our survey, the inner channel was filled with warm, low-salinity estuarine water (temperature >20°C, salinity <31.2 psu). Waters in the outer channel comprised two different water masses: surface water of high temperature (>20°C) and low salinity (31.7–32.0 psu); and bottom water of low temperature (<15°C) and high salinity (>32.2 psu). The cold bottom water originates from the Yellow Sea Cold Water (<10°C), which lies in the lower layer below the seasonal pycnocline in the Yellow Sea at summertime (Lie, 1984). At the westernmost station C05, a strong thermocline was formed around 20 m and the temperature difference between the upper and lower layers exceeded 14°C. In the middle channel, the hydrographic properties were vertically uniform, reflecting the occurrence of almost complete vertical mixing. The sea surface temperature was the lowest at station C00 in the middle channel. The temperature in the lower layer gradually increased landward from the outer channel, while the lower layer salinity gradually increased seaward. The landward increase in temperature and the landward decrease in salinity are proofs of the onshore intrusion of the Yellow Sea Cold Water through the main channel.

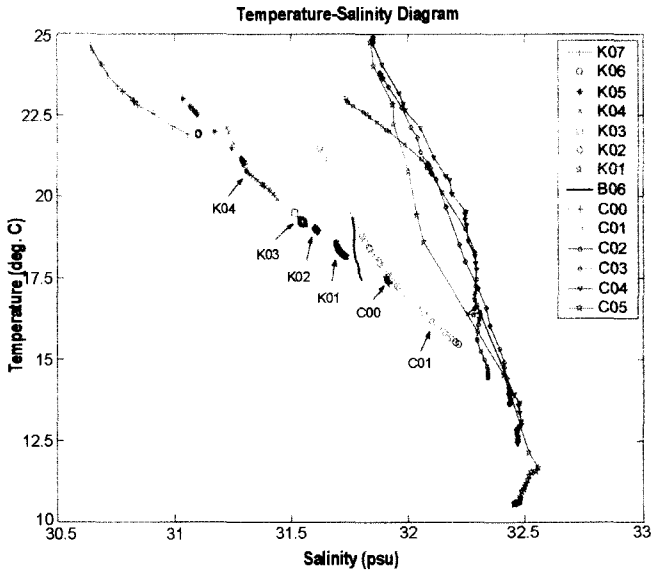

Fig. 3. Temperature-salinity relations in the main tidal channel from July 26 to 29, 1999. Ranges for temperature and salinity are greatly reduced at stations C00 to K03 in the middle channel.

In the outer channel, the seasonal thermocline, halocline, and pycnocline were commonly formed near the 20 m depth. Dense isolines around the pycnocline at stations C04 and C05 tend to diverge toward the well-mixed zone. Isolines in the upper layer intersected the sea surface near station C01 to form a surface front, whereas isolines in the lower layer declined toward the bottom to form a bottom front. The divergent pattern of isolines with the formation of two fronts is the typical structure produced by tidal mixing as observed in many continental shelves (e.g., Simpson and James, 1986; Yanagi and Koike, 1987; Lie, 1989; Cho and Seung, 1989). Temperature-salinity relations in Fig. 3 show a sharp reduction in ranges for temperature and salinity at stations C00 to K03 in the well-mixed zone. The water in the mixed zone is a mixture of estuarine and offshore waters.

Stratification

The potential energy anomaly is a measure of vertical stratification, which is defined as energy requirement per unit volume to bring out complete vertical mixing (Simpson *et al.*, 1977).

$$P = \frac{1}{H}\int_{-H}^{0} (\rho - \bar{\rho}) g\, z\, dz \qquad (1)$$

where H is the water depth, ρ is the density, $\bar{\rho}$ is the vertically averaged density, g is the gravity and z is the vertically upward coordinate from the sea surface. The density is the function of temperature (T), salinity (S) and pressure (p). In coastal water shallower than 100 m, the equation of seawater state can be approximated to a linear equation (e.g., Mamayev, 1975).

$$\rho = \rho_0(1-\beta T+\gamma S) \tag{2}$$

where ρ_0 is some constant value of density, β and γ are coefficients of heat expansion and saline contraction of seawater.

By inserting equation (3) in (1), we obtain

$$P = -\frac{\rho_o}{H}\int_{-H}^{0}\beta(T-\bar{T})g\,z\,dz+\frac{\rho_o}{H}\int_{-H}^{0}\gamma(S-\bar{S})g\,z\,dz \tag{3}$$

The first and second terms on the right hand side correspond, respectively, to contributions of T and S to the potential energy anomaly, P. That is,

$$P = P(T)+P(S) \tag{4}$$

Since the two coefficients β and γ are not linear functions of T and S, it is practical to compute $P(T)$ and $P(S)$ approximately by choosing their representative values for given intervals of temperature and salinity. For the observed intervals shown in Fig. 3, β ranges -0.15 to -0.29×10^{-4}/°C, while γ ranges 0.72 to 0.74×10^{-4}/psu. Therefore, we computed P, $P(T)$, and $P(S)$ along the channel by fixing $\beta = -0.24\times10^{-4}$ /°C and $\gamma = 0.72\times10^{-4}$/psu which are values for $T=$ 20°C and $S=30$ psu and by taking as vertically averaged density at each station. In consequence, $P(T)$ and $P(S)$ do not add up exactly to P.

Fig. 4 shows that the potential energy anomaly is greater than 100 Joules/m^3 in the outer channel where the water column was strongly stratified, but drops sharply to about 2 Joules/m^3 at station C00 in the well-mixed zone. The temperature contribution accounts for larger than 80% of the anomaly in the outer channel. In other words, the stratification in the stratified zone was built up mainly due to a large vertical temperature gradient. The temperature contribution is larger than 75% even in the weakly stratified inner channel, although the anomaly is small with a magnitude of less than 30 Joules/m^3. At stations K02, K03, and K06, the anomaly approaches to zero, indicating the occurrence of almost complete vertical mixing.

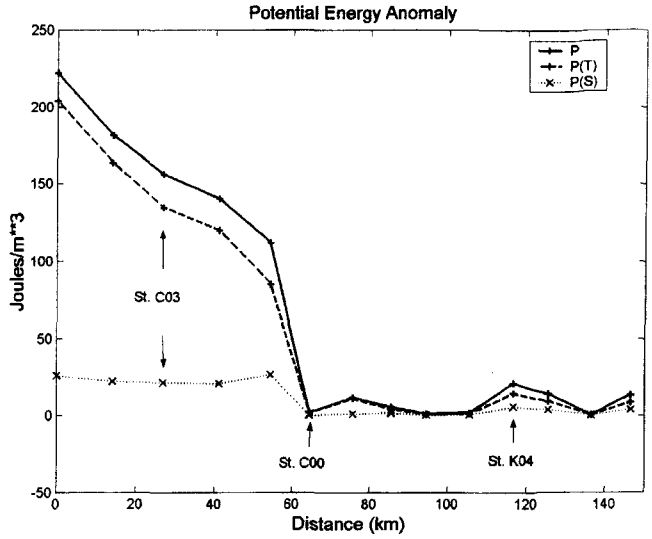

Fig. 4. Potential energy anomalies in the main tidal channel from July 26 to 29, 1999. Solid line, dashed line with Xs, and dashed line with crosses denote the total potential energy anomaly and contributions of temperature and salinity to the anomaly. The two contributions were approximated by choosing constant coefficients of heat expansion and saline contraction for $T=20$°C and $S=30$ psu.

HOURLY VARIATION IN VERTICAL HYDROGRAPHIC STRUCTURE

Vertical hydrographic structure may respond to temporal variations of tidal mixing and tidal advection even over the semidiurnal period, since semidiurnal tidal currents dominate the tide regime. Fig. 5 presents the hourly evolution of vertical profiles of temperature, salinity, and sigma-t at station S01 from 20:00 of July 25 to 08:00 of July 26, 1999. Sea level variations at tidal station Anheung, which is about 25 km away from station S01, are also presented in the bottom panel of Fig. 5. These hourly observations inform us of how the semidiurnal tides affect the vertical hydrographic structure in the main channel. During the observations, low tide (LT) and high tide (HT) at Anheung occurred at around 20:00 of July 25 and 3:00 of July 26, respectively, with a tidal range of about 4 m. Isotherms, isohalines, and isopycnals moved up and down with time. Isolines in the lower layer below 30 m were lowest at LT+3 hours and highest at HT-1 hour. During LT+3 hours and HT-1 hour, isolines in the upper layer including the summer pycnocline, however, changed slightly. Since then, isolines in the upper 40 m moved down from HT-1 to HT+2 hours, but moved up from HT+2 to HT+4 hours, indicating a vertical displacement of

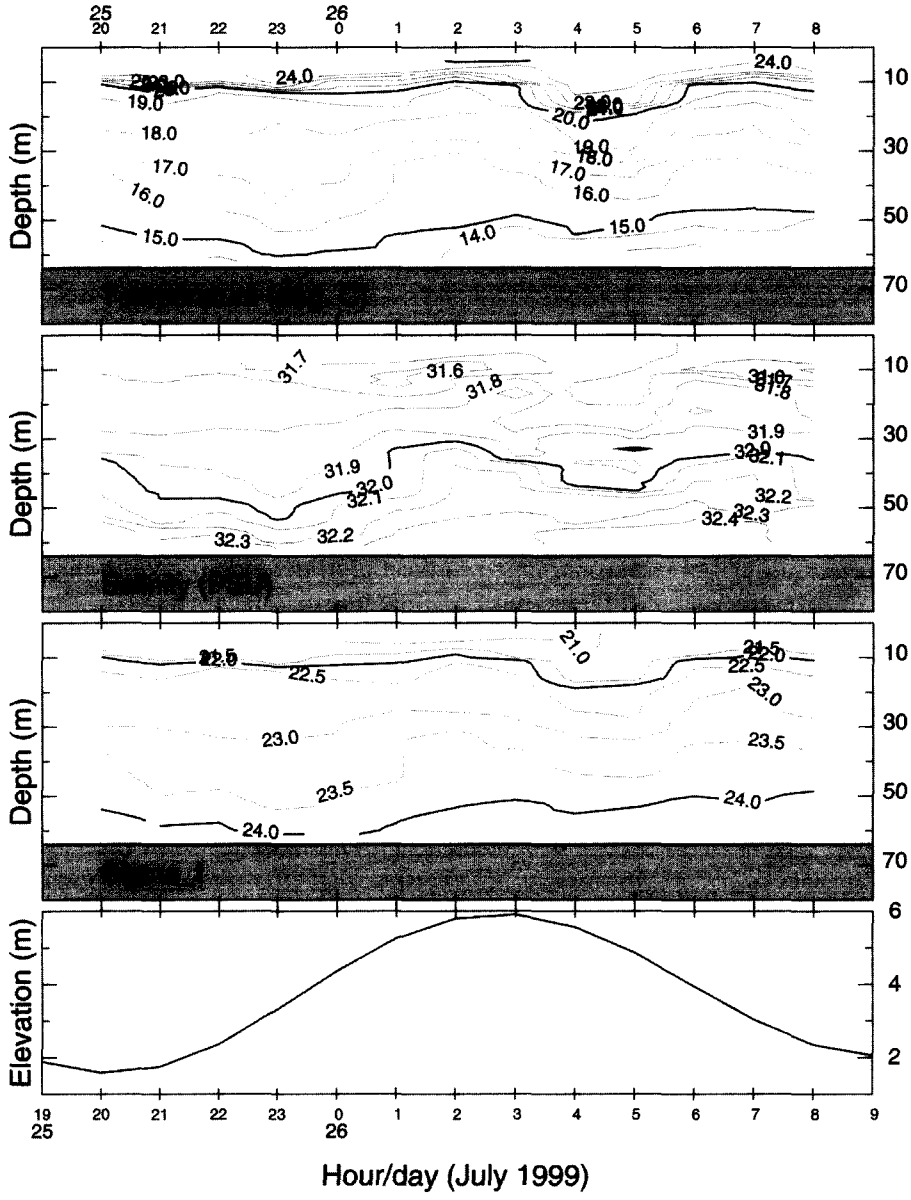

Fig. 5. Hourly variations of temperature, salinity, and sigma-t at station S01 from July 25 to 26, 1999. Sea level changes at Anheung are presented in the bottom panel.

about 10 m. A bowl-shaped pattern of isotherms is clearly seen during HT to HT+3. The vertical displacement for about three hours around the high tide is a peculiar feature observed for the first time in the Korean coastal area.

The total potential energy anomaly computed from the hourly CTD data at St. S01 varied from 45 to 190 Joules/m^3 (Fig. 6). Salinity contribution to the anomaly is less than 35 Joules/m^3, which is smaller than the temperature contribution. This means that the large variation in stratification in the frontal zone was closely associated with the hourly variation in vertical temperature gradient. The stratification was strongest at HT+1 hour at Anheung and was weakest at LT. The second-to-the lowest stratification value was observed at LT+3 hours when isopleths in the lower layer were at their lowest.

Since the tidal phase near station S01 is different from that at Anheung, we compared the hourly variation of the anomaly with tidal currents observed by the GPS drifters. Fig. 7 presents trajectories of the two drifters drogued at 15 m and 40 m which were smoothed by a 30-minute running average. Slack waters after ebb and flood occurred around 21:00 of July 25 and 04:00 of July 26, respectively. The potential energy anomaly peaked around the slack water after flood. During the flood, isopleths below the seasonal pycnocline moved up, but for about three hours

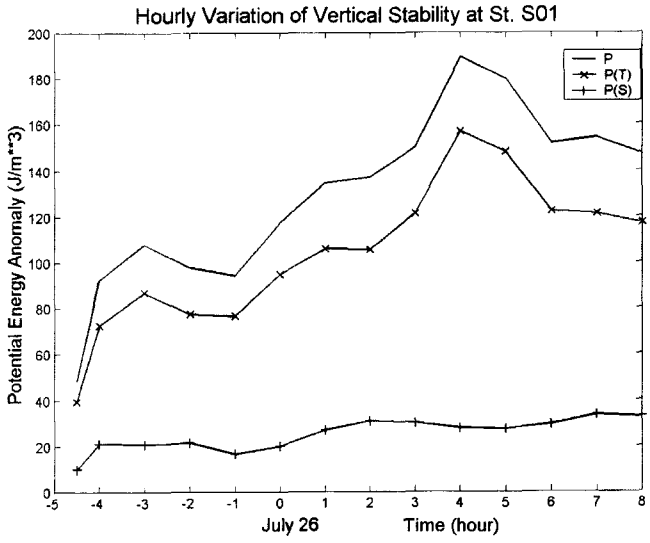

Fig. 6. Hourly variations of the potential energy anomalies at station S01 and along-channel moving velocity of two drifters near station S01 from July 25 to 26, 1999. Solid line, dashed line with Xs, and dashed line with crosses denote the total potential energy anomaly and the contributions of temperature and salinity to the anomaly, respectively. The two contributions were approximated by choosing constant coefficients of heat expansion and saline contraction for $T = 20°C$ and $S = 30$ psu.

around the slack water after flood, a concave of isopleths appeared in the upper 50 m, indicating that warm surface water sank further. The deepening of surface water may be associated with the spatial structure of tidal currents in the main tidal channel, where the cross-section decreases landward. Usually, tidal currents in a tidal channel are stronger at the center of the channel than on the shoals (Valle-Levinson and O'Donnell, 1996). During the flood, a portion of inflow spreads out over the shoals, while during the ebb, a portion of water on the shoals converges toward the channel center. Consequently, such axial convergence of warm water on the shallow shoals may deepen the surface layer in the channel, although further investigations are needed in the future to explain the process in detail using a three-dimensional tide model.

DISCUSSIONS

Position of tidal front

The mean position of a tidal front can be predicted effectively using the Simpson-Hunter mixing parameter. This parameter is usually computed using a numerical tide model, but the spatial complexity of bottom topography and coastline in the Kyunggi Bay requires a very fine model. Instead of developing a model appropriate to the bay, we computed the mixing parameter based on the Lagrangian velocity computed from the observed drifter motions. The difference between the Lagrangian and Eulerian velocities corresponds to the Stokes drift velocity (LeBlond and Mysak, 1978). In a tidal channel several times longer than tidal excursions of the major tidal currents, the currents along the channel are dominant and their phases and amplitudes can be assumed to be spatially uniform over the corresponding tidal excursions. Under this assumption, the Stokes drift velocity associated with the major tidal currents is almost zero, so that the Lagrangian velocity can be approximated to the Eulerian velocity within the spatial extent of a tidal excursion.

Fig. 8 presents temporal variations of the mixing parameter and tidal currents along the channel based on the drifter trajectories. The mixing parameter has minimum value of about 100 $s^3 m^{-2}$ at the flood and ebb and maximum value greater than 10^4 $s^3 m^{-2}$ at the slack waters. Apparently, the observed minimum value is consistent with a model result of Lie (1989), but it is noteworthy that the minimum potential energy anomaly at station S01 did not occur at the flood and ebb. The mismatch in position is due to the fact that the Simpson-Hunter mixing parameter does not consider stratification and temporal variation of tidal currents. Nevertheless, the position of the observed tidal fronts around station C01 in Fig. 2 is fairly consistent with a mixing parameter of about 100 $s^3 m^{-2}$ computed from the maximum drifter velocities, with position error of a tidal excursion.

Effect of tidal advection on stratification

The hourly variation of the potential energy anomaly (Fig. 6) tends to linearly increase from a minimum at the slack water after ebb to a maximum at the slack water after flood. Provided that winds and buoyancy flux through the sea surface are not imposed on the water column, the stratification of the water column depends mainly on tidal advection and/or vertical mixing. If the tidal mixing was responsible for the hourly variation of the potential energy anomaly, the potential energy anomaly should have shown two maximums at the two slack waters within a semidiurnal cycle. Now, we consider the tidal advection in one-dimensional channel. Time

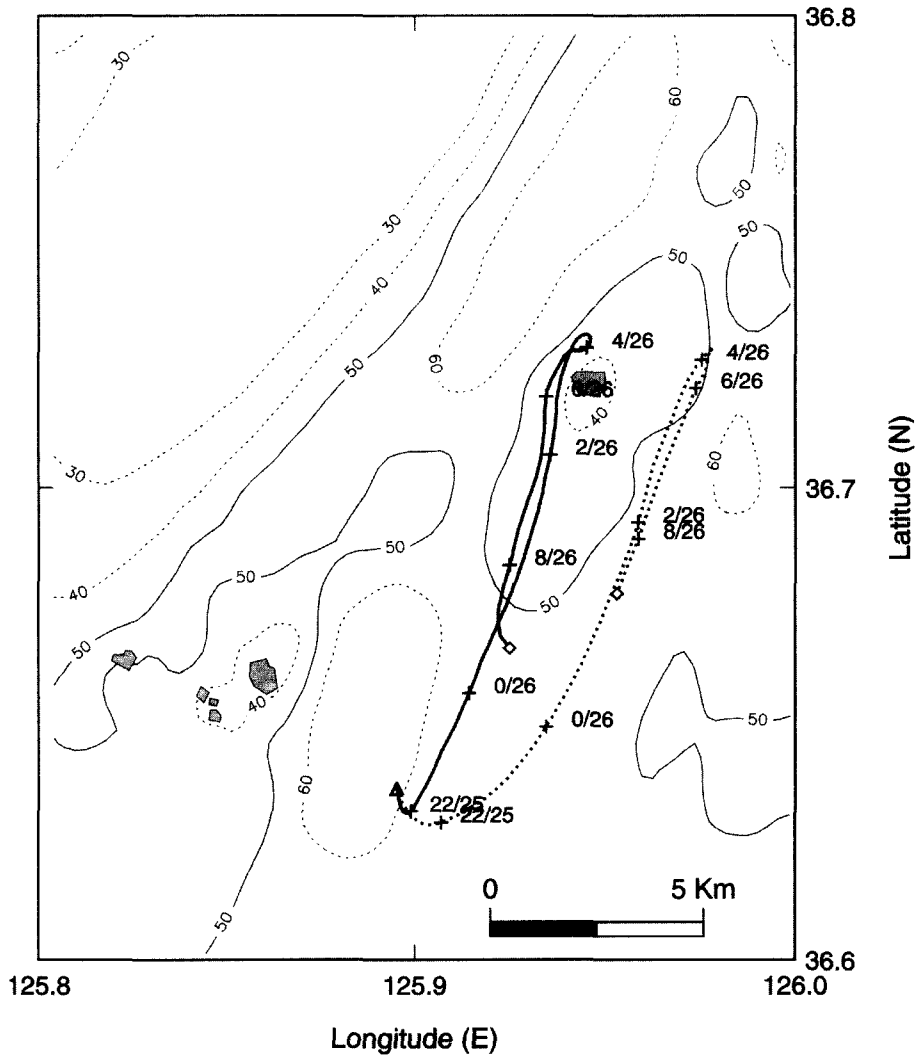

Fig. 7. Trajectories of two GPS drifters drogued at 15 m (solid line) and 40 m (dashed line) from July 25 to 26, 1999. Slack waters occurred around 21:00 of July 25 and 04:00 of July 26. Numerals along the trajectories indicate time (hour/day).

variation of the potential energy anomaly dP/dt at point x is given by $\partial P/\partial x\ dx/dt$. In the tidal frontal zone, $\partial P/\partial x$ is estimated to have a value of 15 Joules/m^3/km from Fig. 4, and the typical tidal excursion is about 10 km from the drifter trajectories (Fig. 7). Hence, the tidal advection satisfactorily accounts for the observed difference in magnitude of about 150 Joules/m^3 between low and high tides. The stratified water column on the offshore side of station S01 is advected landward by the inward flood current, while the water column on the onshore side is advected seaward by the outward ebb current. The tidal front in the main channel thus displaces back and forth over a tidal excursion in the along-channel direction. Of course, front formation is attributed to the tidal mixing, but the hourly variation of the potential energy anomaly is primarily caused by the tidal advection along the channel.

SUMMARY AND CONCLUSIONS

Tidal frontal structure and its hourly evolution in the main tidal channel of the Kyunggi Bay were investigated by analyzing CTD data collected along the channel, hourly CTD data gathered from a fixed point for 13 hours, and GPS drifter trajectories. A tidal front appeared northwest of the Taean peninsula with a mean position that was consistent with about 100 s^3 m^{-2} of the mixing parameter. Hourly variations of the potential energy anomaly in the frontal zone show that stratification was intensified around the slack water after flood, but they became weaker around the slack water after ebb. This variation is primarily caused by the advection of water column along the channel by tidal currents. Consequently, the tidal front displaces on- and offshore in the main channel over a tidal excursion of about 10 km, with

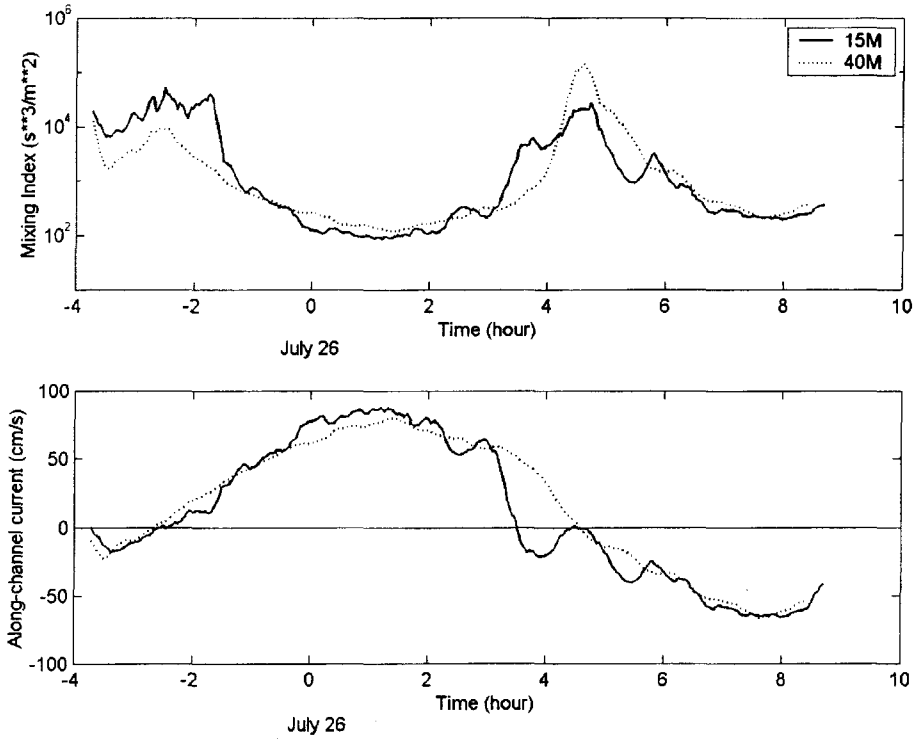

Fig. 8. Hourly variations of the Simpson-Hunter mixing index, H/U^3, and current along the channel estimated using two GPS drifters drogued at 15 m (solid line) and 40 m (dashed line) from July 25 to 26, 1999.

landward advection of stratified water in the offshore area during the flood and seaward advection of less stratified water during the ebb.

In the tidal frontal zone, isolines in the upper 50 m were bowl-shaped for about three hours around the slack water after flood, due to the downward motion of warm surface water. The downward motion which intensifies the stratification may be closely associated with the confluence of warm water on the channel shoals to the channel axis at the beginning of the ebb, although its dynamical process should be investigated further based on intensive surveys both across and along the channel.

ACKNOWLEDGEMENTS

This study is a contribution to the National Research Laboratory for Ocean Prediction of the Yellow and East China Seas, funded by the Korean Ministry of Science and Technology (MOST). Data used were collected through a project, entitled Coastal Ocean Processes for Marine Pollution in the Yellow Sea, which was also supported by MOST. The authors thank the staff of KORDI including the crew members of R/V Eardo who assisted in the field measurements in July 1999. We also thank Dr. K.T. Chung and an anonymous reviewer for their helpful criticisms.

REFERENCES

Cho, C.H. and Y.H. Seung, 1989. An oceanographic survey of tidal front around Kyunggi Bay. *Yellow Sea Res.*, **2**: 51–61.(in Korean)

Choi, H.-Y., S.-H. Lee and I.-S. Oh, 1998. Quantitative analysis of the thermal front in the mid-eastern coastal area of the Yellow Sea. *The Sea, J. Korean Soc. Oceanogr.*, **3**: 1–8. (in Korean)

Choi, J.-Y. and Y.-A. Park, 1998. Southward transport of suspended sediments during summer season in the coastal zone off Tae-An peninsular, west coast of Korea. *The Sea, J. Korean Soc. Oceanogr.*, **3**: 45–53. (in Korean)

LeBlond, P.H. and L.A. Mysak (1978). Waves in the Ocean. Elsevier Sci. Pub. Co., Amsterdam, 602 pp.

Lie, H.-J., 1984. A note on water masses and general circulation in the Yellow Sea (Hwanghae). *J. Oceanol. Soc. Korea,* **19**: 187–194.

Lie, H.-J., 1989, Tidal fronts in the southeastern Hwanghae (Yellow Sea). *Cont. Shelf. Res.*, **9**: 527–546.

Mamayev, O.I., 1975. Temperature-salinity Analysis of World Ocean Waters. Elsevier Sci. Pub. Co., Amsterdam, 374 pp.

National Oceanographic Research Institute, 1998. Tidal current observations in the approaches to Kyongnyolbi Yoldo, In: Technical Reports of Hydrography, Pub. No. 820, pp. 47–63.

Neumann, G. and W.J. Pierson, 1966. Principles of Physical Oceanography. Prentice Hall, Inc., Englewood Cliffs, 545 pp.

Officer, C.B., 1976. Physical Oceanography of Estuaries (and Associated Coastal Waters). John Wiley & Sons, New York, 465 pp.

Park, Y.A., J.Y. Choi, C.B. Lee, D.C. Kim, and K.W. Choi, 1994. Sediment distributions and depositional processes on the inner continental shelf off the west coast (middle part) of Korea. *J. Korean Soc. Oceanogr.*, **29**: 357–365 (in Korean).

Seung, Y.H., J.H. Chung, and Y.C. Park, 1990. Oceanographic

studies related to the tidal front in the mid-Yellow Sea off Korea: Physical aspects. *J. Oceanol. Soc. Korea,* **25**: 84–95.

Simpson, J.H. and J.R. Hunter, 1974. Fronts in the Irish Sea. *Nature,* **250**: 404–406.

Simpson, J.H. and I.D. James, 1986. Coastal and estuarine fronts. In: Baroclinic Processes on Continental Shelves. Edited by C.N.K. Mooers, American Geophys. Union, Washington, D.C.,pp. 63–93

Simpson, J.H., D.H. Hughes, and N.C.G. Morris, 1977. The relation of seasonal stratification to tidal mixing on the continental shelf. In: A Voyage of Discovery, Supplement to*Deep-Sea Res.*, pp. 327–340.

Valle-Levinson, A. and J. O'Donnell, 1996. Tidal interaction with buoyancy-driven flow in a coastal plain estuary. In: Buoyancy Effects on Coastal and Estuarine Dynamics, edited by Aubrey, D.G. and C.T. Friedrichs, American Geophys. Union, Washington D.C., pp. 265–182.

Yanagi, T. and T. Koike, 1987. Seasonal variations in thermohaline and tidal fronts in the Seto Inland Sea, Japan. *Cont. Shelf Res.*, 7: 149–160.

Yi, S.-U., 1972. On the tides, tidal currents and tidal prisms at Inchon Harbor (abstract only in English). *J. Oceanol. Soc. Korea,* 7: 86–97.

Manuscript received August 25, 2001
Revision accepted March 12, 2002
Editorial handling: Dong-Kyu Lee